INTERNATIONAL JOURNAL OF
ENERGY AND ENVIRONMENT

Volume 7, Issue 1, 2016 pp.1-22

Journal homepage: www.IJEE.IEEFoundation.org

A parametric study of the natural vibration and mode shapes of PEM fuel cell stacks

Maher A.R. Sadiq Al-Baghdadi

Fuel Cell Research Center, International Energy and Environment Foundation, Najaf, P.O.Box 39, Iraq.

Abstract

A PEM fuel cell stack is laminated with a number of plate-type cells, and the latest model is assembled by compression from both ends of plates.PEM fuel cells are exposed to high magnitude vibrations, shocks, and cyclic loads in many applications. Vibrations during operation show significant impact in the longer run of the fuel cells. Frequencies which are not close to the resonant frequencies or natural frequencies show very little effect on the overall performance. However, if the frequency ranges of operation approaches the resonant frequency range, the probability of component failure increases. It is possible that there will be lateral transition of cells or leakage of fuel gas and coolant water. Therefore, it is necessary to evaluate the effects vibration has on the fuel cell.

This work aims to understand the vibration characteristics of a PEM fuel cell stack and to evaluate their seismic resistance under a vibration environment. Natural frequencies and mode shapes of the PEM fuel cell stack are modelling using finite element methods (FEM).A parametric study is conducted to investigate how the natural frequency varies as a function of thickness, Young's modulus, and density for each component layer. In addition, this work provides insight into how the natural frequencies of the PEM fuel cell stack should be tuned to avoid high amplitude vibrations by modifying the material and geometric properties of individual components. The mode shapes of the PEM fuel cell stack provide insight into the maximum displacement exhibited under vibration conditions that should be considered for transportation and stationary applications.

Keywords: Free vibration; Natural frequency; Mode shapes; PEM fuel cell; Composite layers.

1. Introduction

Recently, PEM fuel cells have attracted attention as new power resources and are used in fuel-cell vehicles and stationary cogeneration systems [1-3]. The PEM fuel cell stack in the power generation parts of inside these appliances has structures laminated with a number of plate-type cells. Since fuel cells operate at less than 100% efficiency, the voltage output of one cell is less than 1.16 volt. Most applications require much higher voltages than this, therefore the required voltage is obtained by connecting individual single fuel cells in series to form a fuel cell stack.

The first step in designing a fuel cell stack is to determine its active area and number of cells in the stack. When a stack is designed for an application, the design inputs come from the application requirements, such as desired power output, desired or preferred stack voltage or voltage range, desired efficiency, and volume and weight limitations. Some of these requirements may conflict each other, and the stack sizing

and design process often results in a compromise solution that meets the key requirements (such as power output) and finds an optimum between the conflicting requirements [4, 5].
PEM fuel cell stacks may be subject to vibrations under dynamic situations found in transportation applications as well as stationary applications near heavy traffic and rail transport. Passenger vehicles generally experience vibrations in the range of 8-16 Hz due to the unevenness of the road and the oscillation of the axel and wheel with the suspension system. PEM fuel cell stacks may be employed to power auxiliary devices in semi-trailers, which typically experience vibrations in the range of 0.9-5.8 Hz during highway driving conditions. Buildings near busy roads are also subject to vibrations due to nearby traffic, which cause vibrations between 5 and 25 Hz. When placed in applications such as these, the PEM fuel cell stack may vibrate at an excitation frequency within the band of its natural frequencies and cause the PEM fuel cell to vibrate in resonance with high amplitude. Therefore, it is critical to identify the natural frequencies that a PEM fuel cell stack may experience in the context of the excitation frequencies expected in these applications. Vibrating at resonance frequency can lead to the initiation and acceleration of defect formation, which may ultimately result in operational failure. Vibrations may exacerbate defects such as pinholes, cracks, and delamination, which can result in fuel crossover, performance degradation, and reduced durability [6-8]. Vibration characteristics are required to understand the vibration behaviour of PEM fuel cell stack components such as the membrane, catalyst layers, gas diffusion layers, bi-polar plates, current plates, gaskets, and end plates.
Rajalakshmi et al. [9] subject a PEM fuel cell stack to vibrations, which include random and swept-sine excitations on a vibrating platform in three axes. Although changes to the mechanical integrity of the stack are not detected, they find a compression force release at the bolts.
Ozgur [10] performsmodal analysis with experimental vibration investigations on an automotive fuel cell stack module in order to design a mounting bracket. They employ an electro-dynamic shaker test apparatus to identify the appropriate mounting system under resonance frequency considerations.
Betournay et al. [11] experimentally investigate the effects of mining conditions on the performance of a PEM fuel cell. They determine the effects of shocks and vibrations on the performance of PEM fuel cell and the effects of mineral and diesel particulate matter on the physical reliability/integrity of the fuel cell stack. They also evaluate the physical reliability/integrity of the fuel cell stack when mounted over the rear wheel of a mine loader chassis, which applied shocks and vibrations to the fuel cell.
PEM fuel cell stack testing has been recently studied in the framework of a European Union harmonized fuel cell testing protocol [12], which is comprised of 55 European partners. Fuel cell testing protocols include the application of vibrations and shocks with 6 degrees of freedom at a frequency of up to 250 Hz.

2. Vibration modeling
The fundamental governing equation for forced vibrations of a structure is written as [6]:

$$[M]\{\ddot{x}\}+[C]\{\dot{x}\}+[K]\{x\}=\{F\} \tag{1}$$

where [M], [K], [C], {x}, are the mass matrix, stiffness matrix, damping coefficient matrix, and displacement matrices, respectively. F is the external excitation force.

Modelling and simulations at the early stage of the stack architecture development are mandatory to lower the costs of the stack and to contribute in designing component dimensions and forms, particularly of stamped bipolar plates or clamping systems. A five cells stack with clamping plate and rod assembly is shown in Figure 1.
The five cells stack model simulated includes the following components; two end-plates, two current plates, and in each cell includes; two bi-polar plates, two GDLs, two gaskets and, an MEA (Figure 2). Material properties and dimensions of each component are shown in Table 1.

3. Results
Vibration characteristics are required to understand the vibration behaviour of PEM fuel cell stack components such as the membrane electrode assemblies, gas diffusion layers, bi-polar plates, current plates, and end plates. Vibrating at resonance frequency can lead to the initiation and acceleration of defect formation, which may ultimately result in operational failure.

The governing equations were discretized using a finite-element method and solved using an academic edition of a multi-physics finite element analysis package. Stringent numerical tests were performed to ensure that the solutions were independent of the grid size. A computational quadratic mesh consisting of a total of 31896 domain elements and 7278 boundary elements was found to provide sufficient spatial resolution (Figure 3). The coupled set of equations was solved iteratively, and the solution was considered to be convergent when the relative error was less than 1.0×10^{-6} in each field between two consecutive iterations.

The assembly conditions are set to reference temperature 20 C, and relative humidity 30%, where the thermal strain of the all stack components and the swelling strain of the membrane are equals to zero. The clamping forces of the nut and bolt are applied on a specific area of the end plates in the assembly procedure. The natural frequencies and the mode shapes of the PEM fuel cell stack are shown in Figure 4 at the base case conditions.

A parametric study is performed to investigate the mechanical and geometrical property effects on the vibration characteristics of a PEM fuel cell stack. Results with deferent conditions are discussed in the following subsections. In the following subsections only the parameter investigated is changed, all other parameters are at the base case conditions as outlined in Table 1.

3.1. Effect of material properties of the stack components

The PEM fuel cell stack is a sandwich-like structure composed of many layers, materials and interfaces. The pressure distribution in PEM fuel cell stack therefore is affected by the component material properties, geometrical parameters and the clamping method. The effect of material variations on the stack layers pressure distribution is identified.

Bipolar plates have traditionally been fabricated from high-density graphite on account of its superior corrosion resistance, chemical stability, high thermal conductivity, and availability. However, due to its molecular structure, it exhibits poor mechanical properties, high manufacturing cost, and it is difficult to work with. Nevertheless, graphite has established itself as the benchmark material for fabrication of bipolar plates, against which all other materials are compared. However, it is not suitable for either transportation applications that require good structural durability against shock and vibration or large-scale manufacturing because of its poor mechanical strength. The thickness of the graphite plates cannot be reduced, resulting in bulkiness and heaviness. As a result, recent studies have moved away from graphite in the direction of developing and optimizing more cost effective materials such as metals and composites.

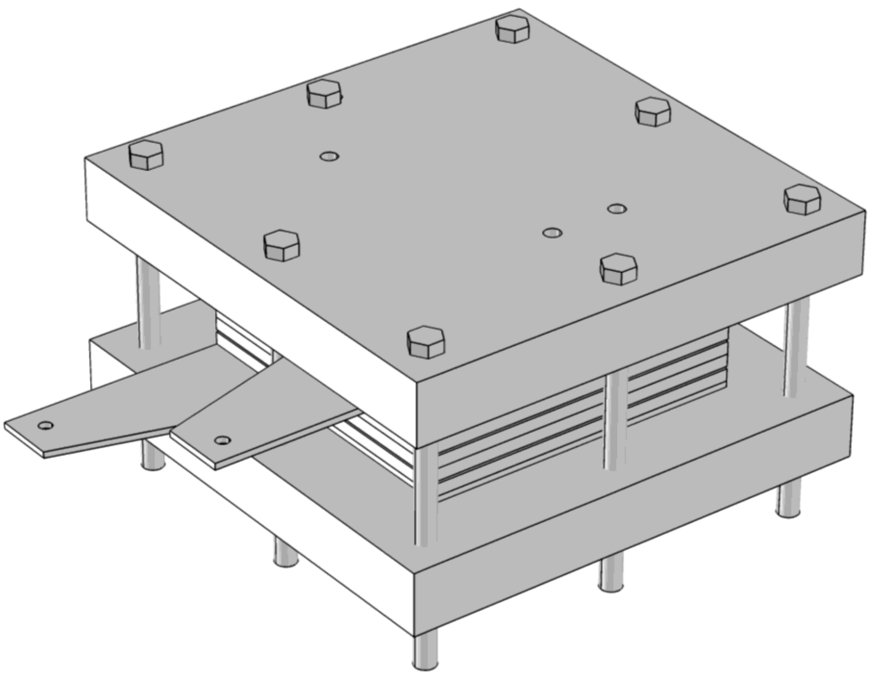

Figure 1. A PEM fuel cell stack assembly.

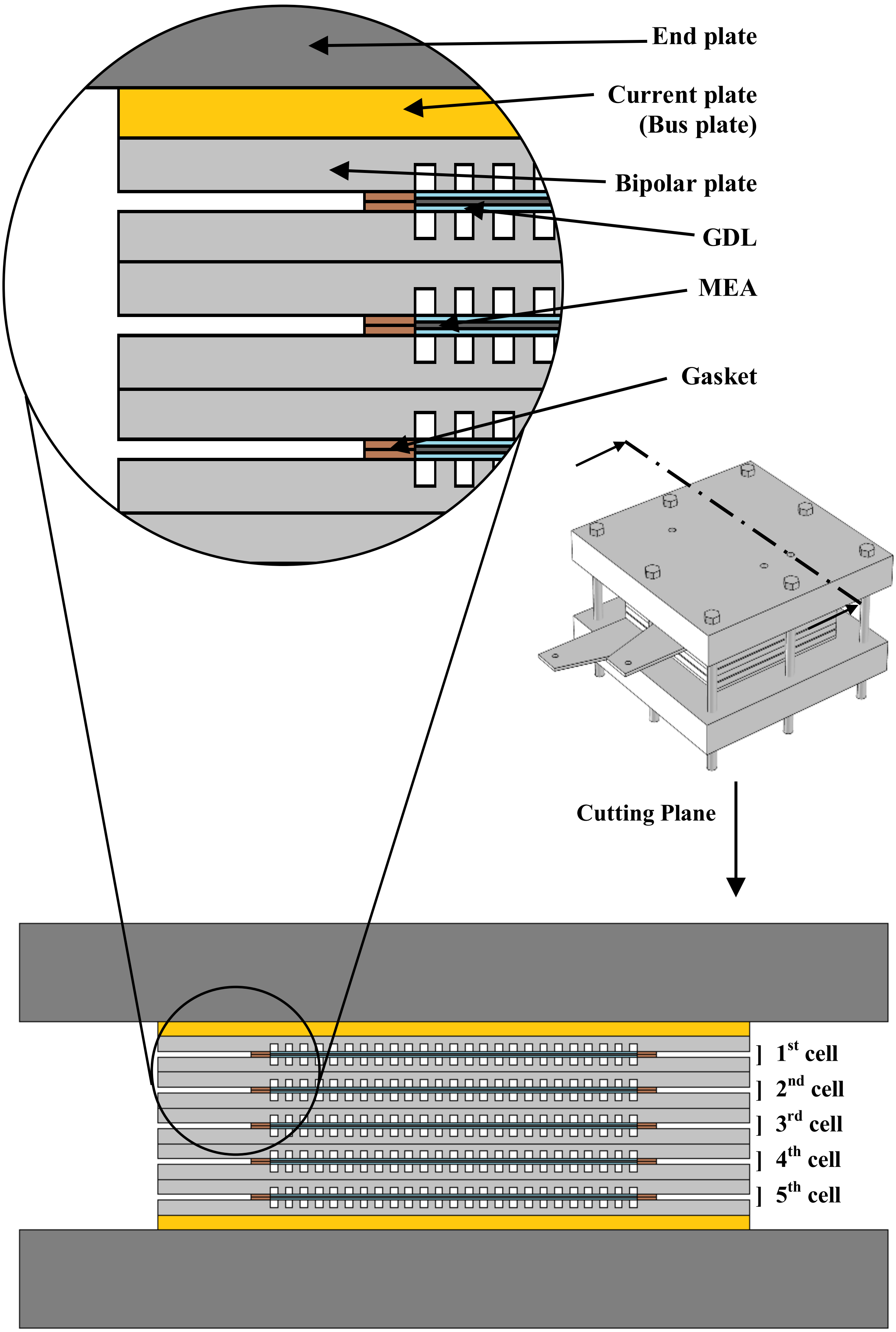

Figure 2. Description of the different stack components (Five cells).

Table 1. Properties of the stack components at base case conditions.

Property	**MEA**	**GDL**	**Bipolar plate**	**Current collector**	**Gasket**	**End plate**
Material	Nafion®	Carbon paper	Carbon graphite	C15720 copper	Taconic®	Stainless steel
Young's modulus [GPa]	Table 2	10	10	110	30	209
Density [kg/m^3]	2000	400	1800	8700	2336	7800
Poisson's ratio	0.25	0.25	0.25	0.35	0.364	0.25
Expansion coefficient [K^{-1}]	123e^{-6}	-0.8e^{-6}	5e^{-6}	17e^{-6}	62e^{-6}	12e^{-6}
Conductivity [W m^{-1} K^{-1}]	0.455	17.122	95	385	0.517	44.5
Specific heat [J kg^{-1} K^{-1}]	1050	500	750	385	932	460
Dimensions [mm]	60 x 60	50 x 50	80 x 80	80 x 80	60 x 60	116 x 116
Thickness [mm]	0.24	0.26	2	2	0.26	13

Table 2. Young's modulus at various temperatures and humidities of Nafion®.

Young's modulus [MPa]	**Relative humidity [%]**			
	30	**50**	**70**	**90**
T=25 C	197	192	132	121
T=45 C	161	137	103	70
T=65 C	148	117	92	63
T=85 C	121	85	59	46

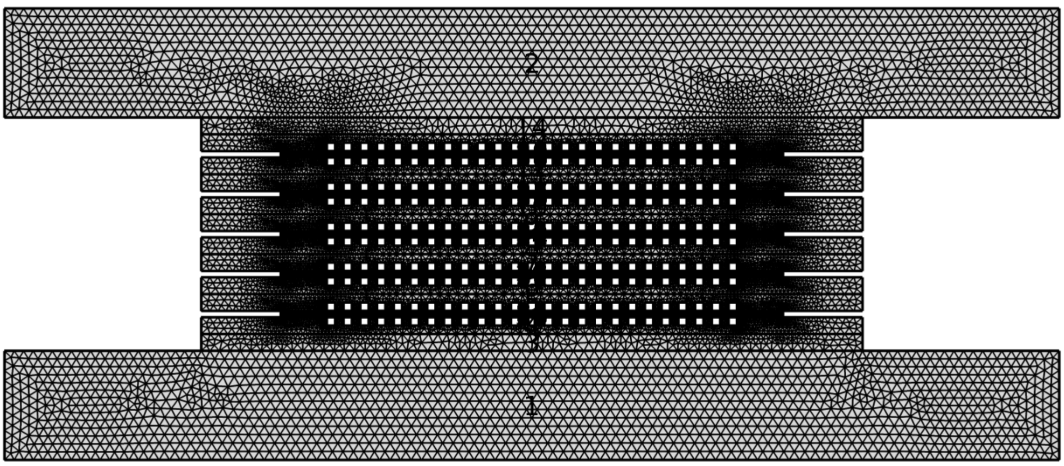

Figure 3. Computational mesh of a PEM fuel cell stack.

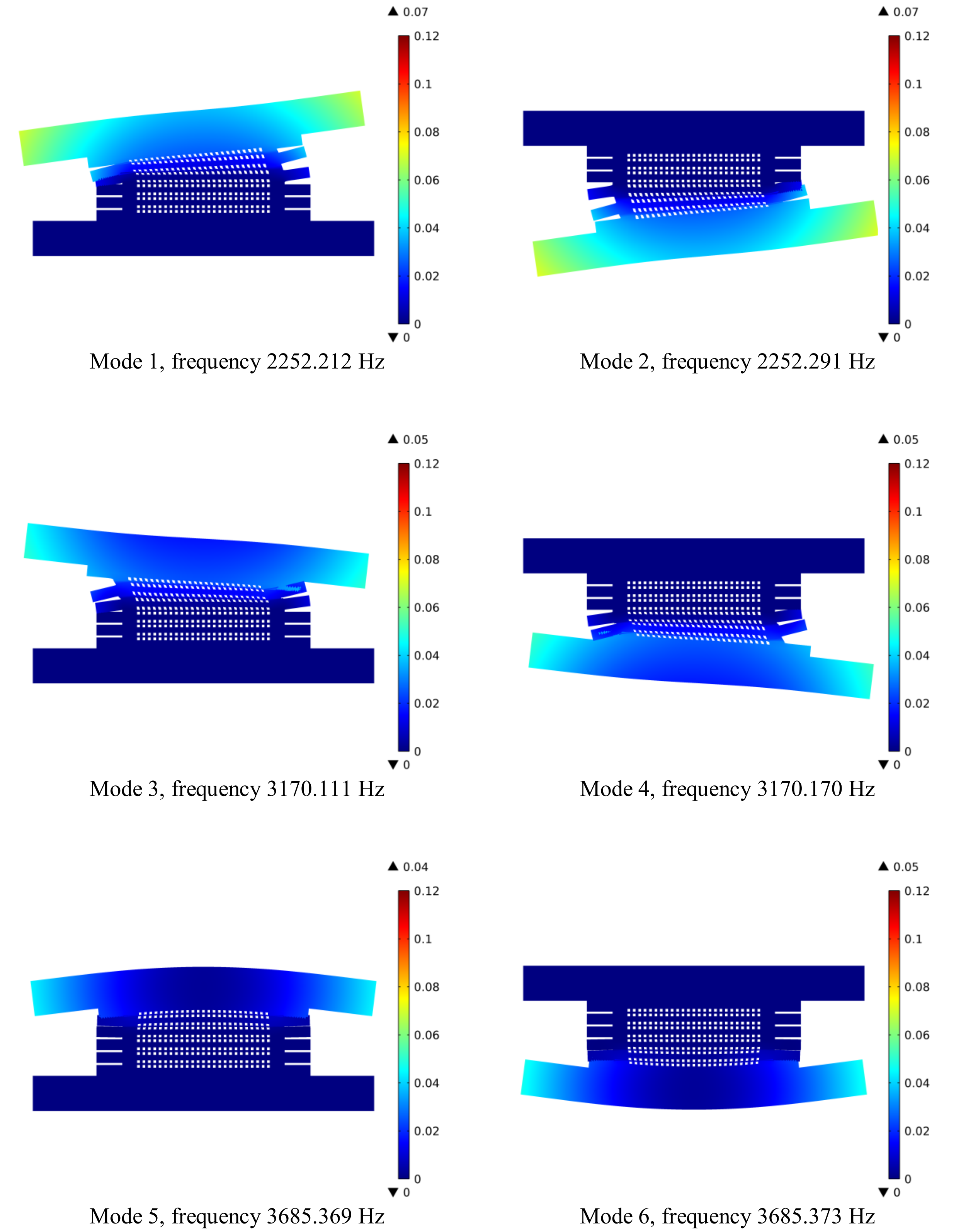

Figure 4. First six natural mode shapes with total displacement [nm].

Metallic materials are another choice for bipolar plates because of their good mechanical strength, high electrical conductivity, high thermal conductivity, high gas impermeability, low cost, and ease of manufacturing. The most advantage of metallic bipolar plates is stamp ability and reducing the thickness plate. Metallic bipolar plates can significantly reduce the volume of fuel cell stacks. In addition, relatively simple fabrication process of gas channels on the metallic plates by stamping enables mass production. In spite of these technical benefits, metallic plates are highly susceptible to corrosion which is closely related to reliability and durability of fuel cell engines. Recently, polymerecarbon composite bipolar plates have been investigated due to their lower cost, less weight, and higher corrosion resistivity in comparison with available materials such as graphite or metallic bipolar plates. The disadvantages of composite bipolar plates are non-stampability, lower electrical and mechanical properties than those of metallic bipolar plates. The effects of changing bipolar plate material are shown in Figure 5.

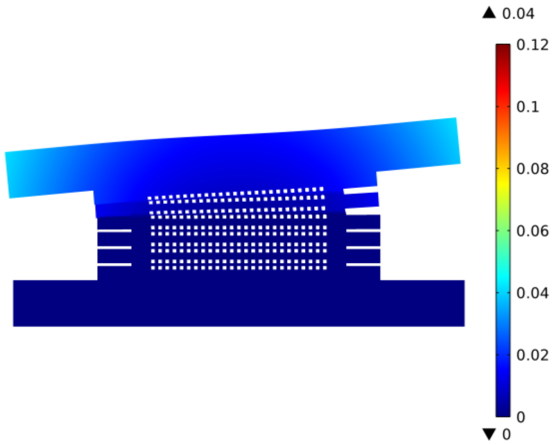

Mode 1, frequency 2892.758 Hz

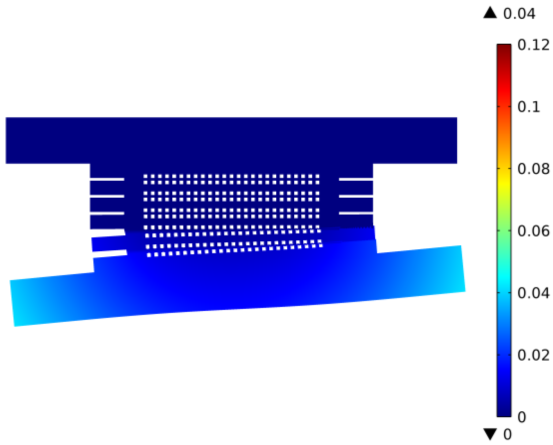

Mode 2, frequency 2892.777 Hz

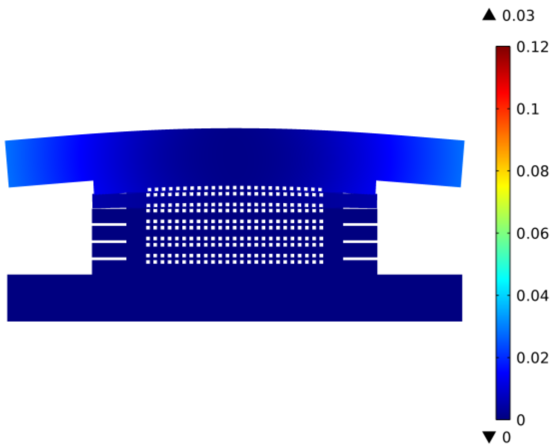

Mode 3, frequency 4279.402 Hz

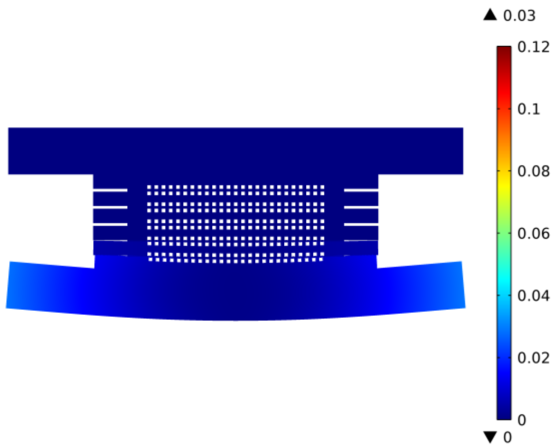

Mode 4, frequency 4279.432 Hz

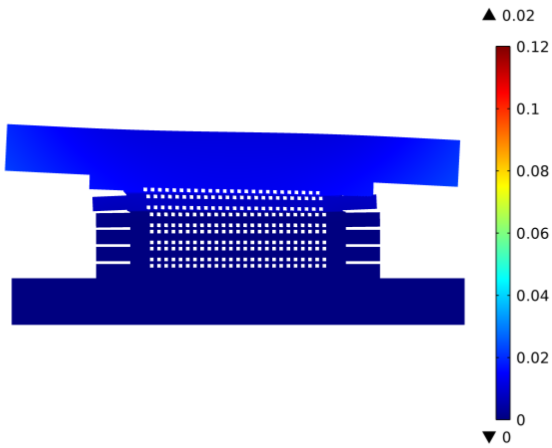

Mode 5, frequency 4342.329 Hz

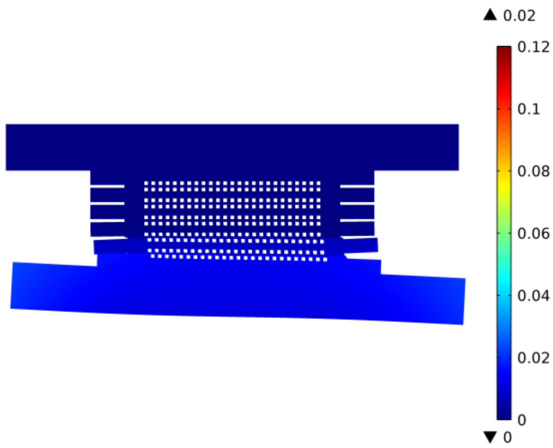

Mode 6, frequency 4342.361 Hz

Figure 5. First six natural mode shapes with total displacement [nm]. (Metallic bipolar plate (SS316L):Young's modulus = 197 GPa; Density = 7800 kg/m^3; Poisson's ratio = 0.3).

Each type of GDL material has its own optimal clamping pressure, to achieve a proper and uniform pressure distribution inside the stack. The inhomogeneous compression of the GDL leads to several opposing effects. On one hand, the assembly pressure improves both electric and thermal conductivities by reducing bulk and contact resistances. Slight compressions may also reduce mass transport resistance due to the shortening of the diffusion path to be covered by the reactants and products in their way to/from the catalyst layers. However, excessive compression loads may impede reactant and product transport due to the loss of pore volume, which is typically, accompanied by a reduction of the effective species diffusivities. On top of that, excessive assembly pressures are known to damage typical paper type GDLs, induce local delamination of the GDL under the channel, and result in non-uniform compressive loads which may degrade the membrane. Pore size reduction may also affect multiphase capillary transport phenomena in the GDL (liquid water removal in PEM fuel cells). And last, but not least, partial GDL intrusion into the channel produces a reactant flow rate reduction or, alternatively, an increase of the parasitic power required to maintain the flow, which affects the overall efficiency of the stack. The effects of changing GDL material are shown in Figure 6.

An important part of the fuel cell is the electrolyte, which gives every fuel cell its name. At the core of a PEM fuel cell is the polymer electrolyte membrane that separates the anode from the cathode. The desired characteristics of PEMs are high proton conductivity, good electronic insulation, good separation of fuel in the anode side from oxygen in the cathode side, high chemical and thermal stability, and low production cost.One type of PEMs that meets most of these requirements is Nafion®. Nafion® membranes come extruded in different sizes and thicknesses. They are marked with a letter N, followed by a 3- or 4-digit number. The first 2 digits represent equivalent weight divided by 100, and the last digit or two is the membrane thickness in mills. The protonic conductivity of a polymer membrane is strongly dependent on membrane structure and its water content. Water uptake results in the membrane swelling and changes its dimensions, which is a very significant factor for fuel cell design and assembly. The dimensional changes are in the order of magnitude of 10%, which must be taken into account in cell design and during the installation of the membrane in the cell. The thickness of the membrane is also important, since a thinner membrane reduces the ohmic losses in a cell. But, if the membrane is too thin, hydrogen, which is much more diffusive than oxygen, will be allowed to cross-over to the cathode side and recombine with the oxygen without providing electrons for the external circuit.

The hot-pressed assembly of the membrane and the catalyst is called the Membrane-Electrode-Assembly (MEA). The catalyst layer is the layer where the electrochemical reactions take place. More precisely, the electrochemical reactions take place on the catalyst surface. Because there are three kinds of species that participate in the electrochemical reactions, namely gases, electrons and protons, the reactions can take place on a portion of the catalyst surface where all three species have access. Electrons travel through electrically conductive solids, including the catalyst itself, but it is important that the catalyst particles are somehow electrically connected to the substrate. Protons travel through ionomer; therefore the catalyst must be in intimate contact with the ionomer. And finally, the reactant gases travel only through voids; therefore the electrode must be porous to allow gases to travel to the reaction sites. At the same time, product water must be effectively removed; otherwise the electrode would flood and prevent oxygen access. Several methods of applying the catalyst layer to the gas diffusion electrode have been reported. These methods are spreading, spraying, and catalyst power deposition. For the spreading method, a mixture of carbon support catalyst and electrolyte is spread on the GDL surface by rolling a metal cylinder on its surface. In the spraying method, the catalyst and electrolyte mixture is repeatedly sprayed onto the GDL surface until a desired thickness is achieved. The effects of changing MEA material are shown in Figure 7.

In a fuel cell, gaskets are normally used to generate the insulation of anodic and cathodic compartments and to avoid gas cross over. Generally, they form a frame around MEA in the un-active zone of the flow field. Because the cell plates are subject to a compression, the gasket material can influence the cell performance and durability. The use of different gasket materials changes the contact pressure distribution on the GDL, affecting the fuel cell performance and lifetime. Moreover, because of the gaskets are typically placed between the bipolar plates and the MEA to guarantee a good sealing, the chemical and mechanical characteristics and stability of the gasket materials must be investigated. In fact these properties are critical for both sealing and the electrochemical performance of the cell. The effects of changing gasket material are shown in Figure 8.

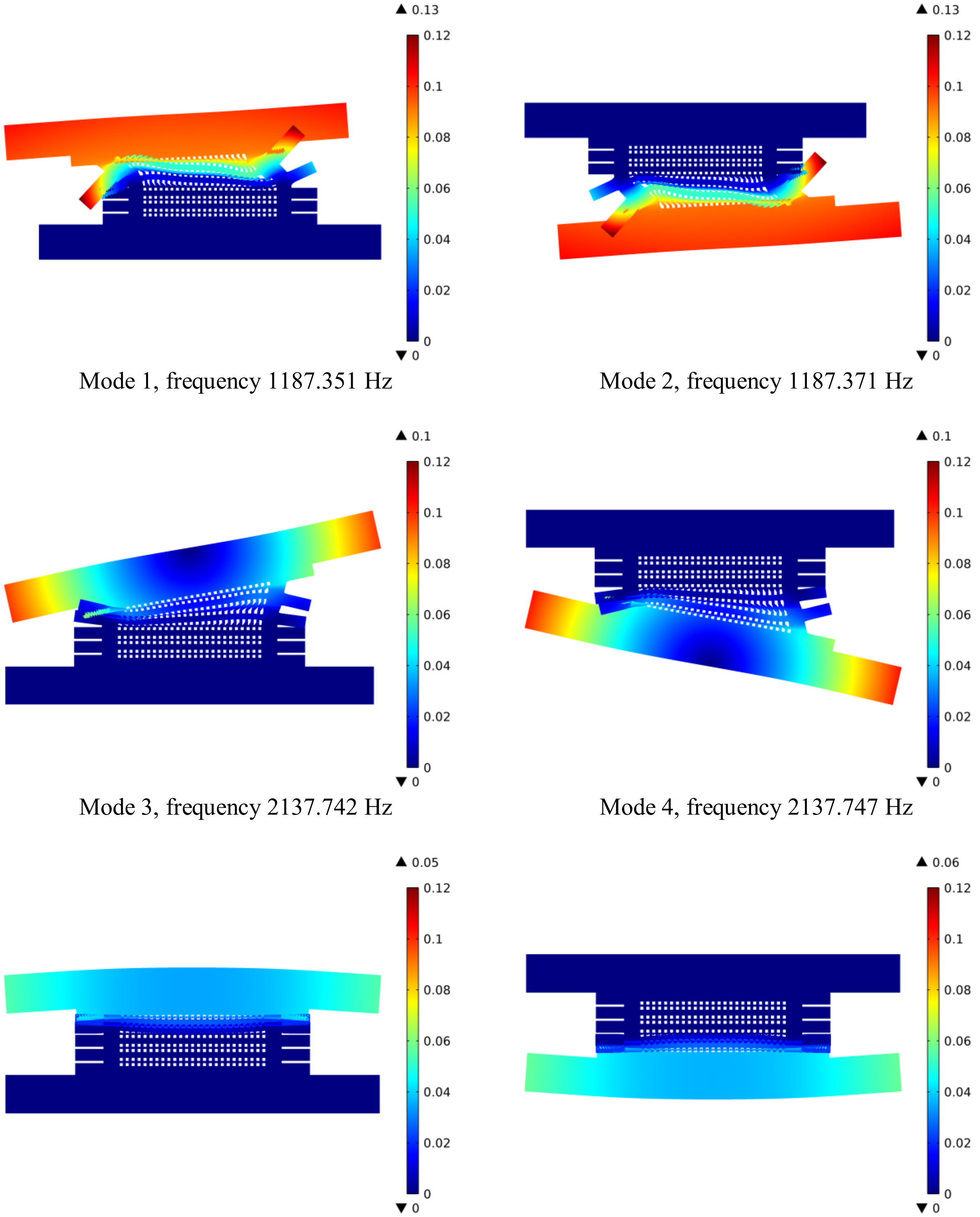

Mode 1, frequency 1187.351 Hz

Mode 2, frequency 1187.371 Hz

Mode 3, frequency 2137.742 Hz

Mode 4, frequency 2137.747 Hz

Mode 5, frequency 2699.062 Hz

Mode 6, frequency 2699.071 Hz

Figure 6. First six natural mode shapes with total displacement [nm]. (GDL (Toray TGP-H-030):Young's modulus = 0.0061 GPa; Density = 440 kg/m^3; Poisson's ratio = 0.1).

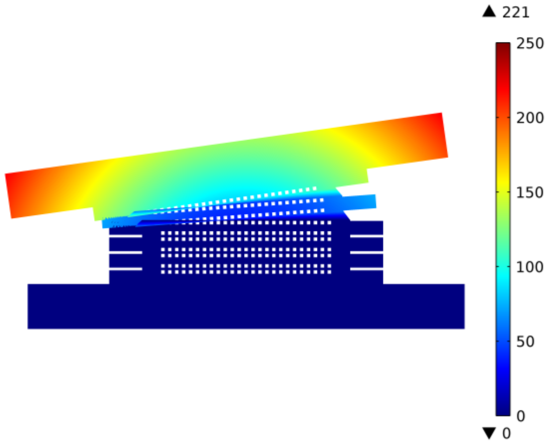

Mode 1, frequency 33.41972 Hz

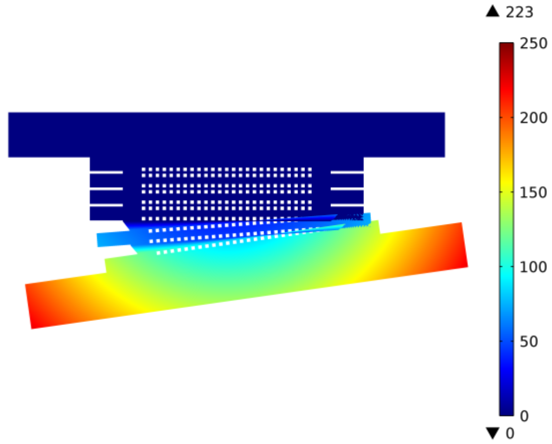

Mode 2, frequency 33.41973 Hz

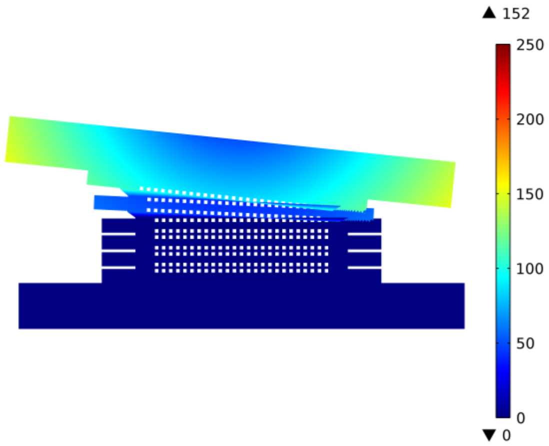

Mode 3, frequency 47.506282 Hz

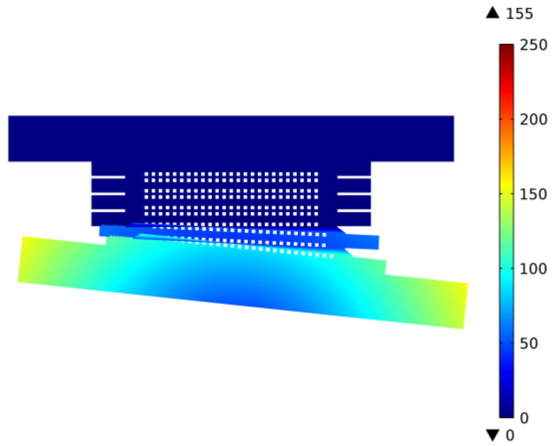

Mode 4, frequency 47.506285 Hz

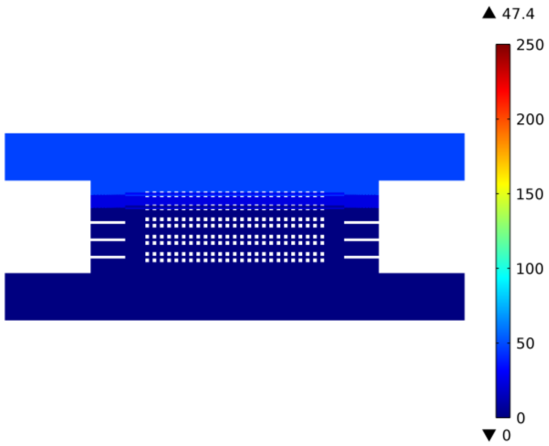

Mode 5, frequency 80.282731 Hz

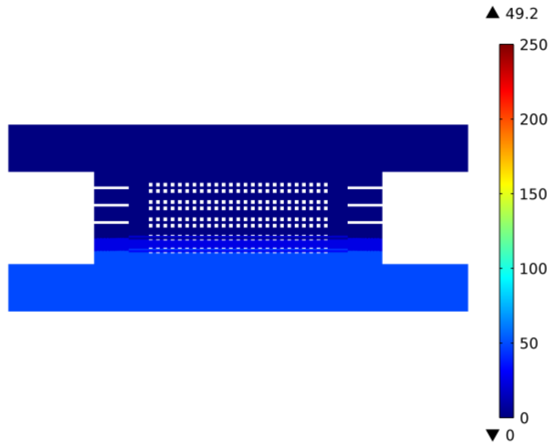

Mode 6, frequency 80.282737 Hz

Figure 7. First six natural mode shapes with total displacement [nm]. (MEA: Young's modulus = 0.02 GPa; Density = 918 kg/m^3; Poisson's ratio = 0.33).

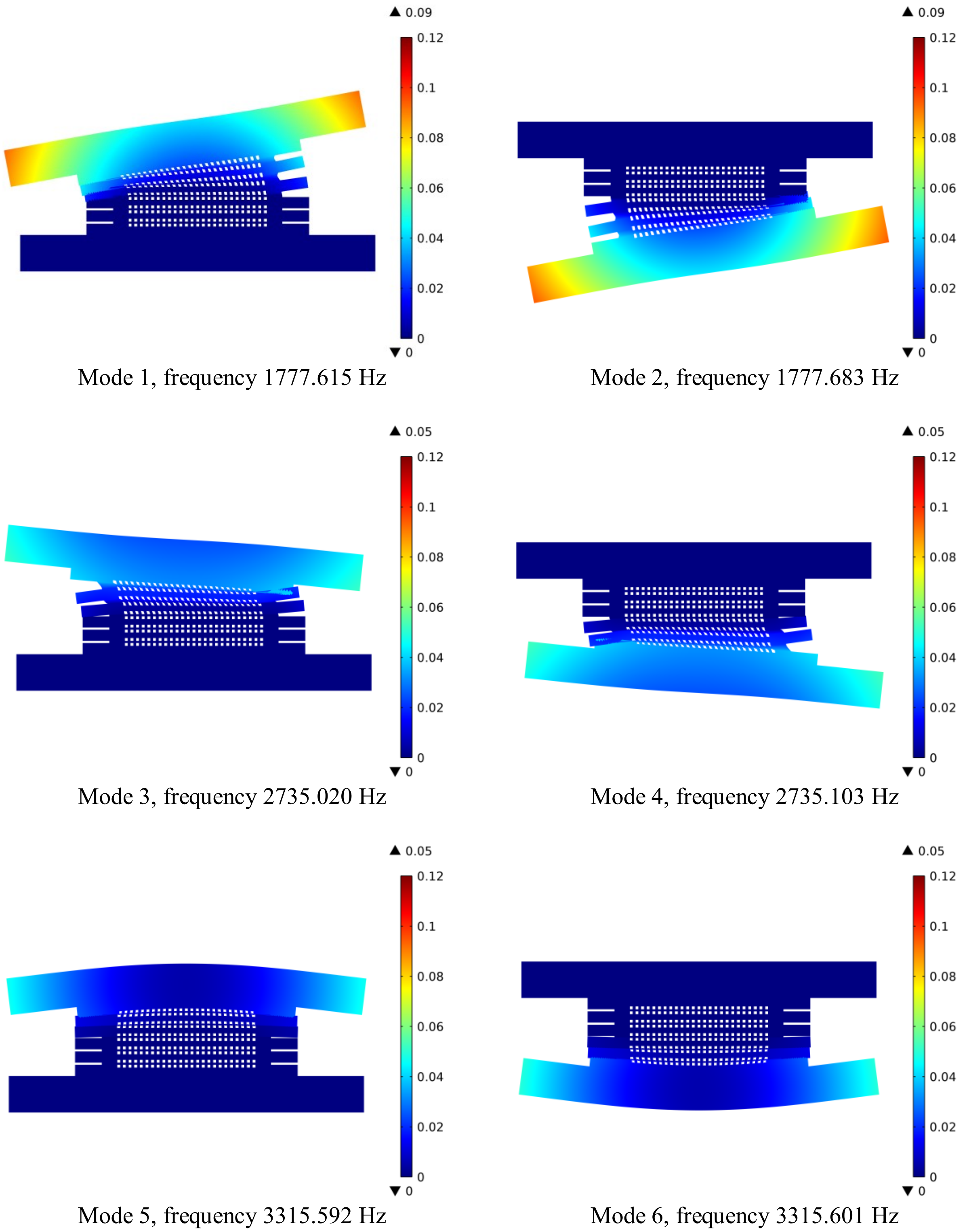

Figure 8. First six natural mode shapes with total displacement [nm]. (Gasket (Rubber (NBR)):Young's modulus = 0.1 GPa; Density = 1286 kg/m^3; Poisson's ratio = 0.33).

The current output terminal sends out the electric current generated by the PEM fuel cell single cell or stack. Current plates for all kinds of fuel cell stacks are made of noble metals such as gold or platinum, or non-noble metals such as stainless steel, copper, or aluminum. The noble metals not only have good conductivity but also can almost avoid electrochemical corrosion and thus will not produce metallic ions that may poison the fuel cell. However, these noble metals are very expensive. The effect of changing current plates material are shown in Figure 9.

The end plate material has a large influence on the mechanical properties of the end plate. A good end plate material has a high Young's modulus and a low density. Possible materials for end plates include, for example, steel, aluminum, and composite materials. If the end plate functions only as a supporting structure, other qualities such as corrosion characteristics or electric properties can be ignored, and the better choice of these materials is the one that at a certain mass makes a more rigid end plate than the other one. The effects of changing end plate material are shown in Figure 10.

3.2. Effect of thickness of the stack components

One of the key elements affecting PEM fuel cell stack performance is the GDL, which must provide a passage for reactant access and excess product removal to/from the catalyst layers, high electronic and thermal conductivity, and adequate mechanical support for the MEA. In order to fulfil these requirements, GDLs are typically made of highly porous carbon-fiber paper or cloth. The high porosity of these materials provides to the GDL a characteristic soft and flexible structure, susceptible of large deformations when subjected to compression. This leads to significant changes in its mechanical, electrical and thermal properties (thickness, porosity, permeability, electrical and thermal bulk conductivities and contact resistances, etc.), thus affecting mass, charge, and heat transfer processes, fuel cell performance and lifetime.

Another key components in the cell assembly are the gaskets. It was found that there is an optimal difference in thickness between gaskets and GDL, in order to prevent problems related to an excessive GDL compression [4, 5]. Mismatch may lead to the following problems: (i) Thinner gasket may lead to sealing problem causing safety issue. In addition to that, the cell will be facing mass transport related losses. (ii) On the other hand, thicker gasket may result in poor contact between the bipolar plate and the GDL, which will be reflected on the ohmic region of the current voltage characteristics [13].

Figure 11 shows that the natural mode shapes and the frequencies of the fuel cell stack was greatly influenced by the thickness difference between the gas diffusion layers and the gaskets, which indicates that a careful design of the assembly is needed to achieve a reasonably good performance for a conventional fuel cell stack.

In a conventional PEM fuel cell stack design, end plates are the two outermost components in a fuel cell assembly. They act as part of the clamping system to provide compressive force in order to unitize the single fuel cells together to form a stack. In addition, they also have some other important functions, such as ensuring good electrical contact between multiple layers within the fuel cell, ensuring good sealing at various interfaces, providing passages for the reactants, products and possibly cooling agents to enter and leave the fuel cell. Although the current design of fuel cell end plates can provide the above listed functions in a somewhat satisfactory manner, it is recognized that there are some existing problems to be solved, such as: deformation of end plates has an influence on fuel cell performance and is difficult to control; end plates are typically bulky and heavy, as compared to the fuel cell stacks; tie rods tend to loosen up during service. This may cause leakage, bad electrical contacts and deteriorated performance of the fuel cell stacks; and repeatability in pressure distribution can hardly be realized among the fuel cell stacks. Figure 12 shows the natural mode shapes and the frequencies of the PEM fuel cell stack with thicker end plates.

3.3. Effect of number of cells in the stack

Increasing the cell active area raises the cell power output, reduces the number of cells required to produce a given plant/system power output, and thus can reduce the cost of electricity, as long as the cell manufacturing yield and cell reliability are not adversely affected. Increasing the number of cells in a stack increases the voltage, while increasing the surface area of the cells increases the current.

In a stack, the compression differences between end cells and middle cells are unavoidable. The more uneven pressure distribution in end cells can lead to reduced gas flows, which usually results in increased flooding. Increasing the number of cells enhances the uniformity of the mechanical state. The better contact pressure homogeneity is obtained with the greater number of cells. Figures 13 and 14 showing this effect.

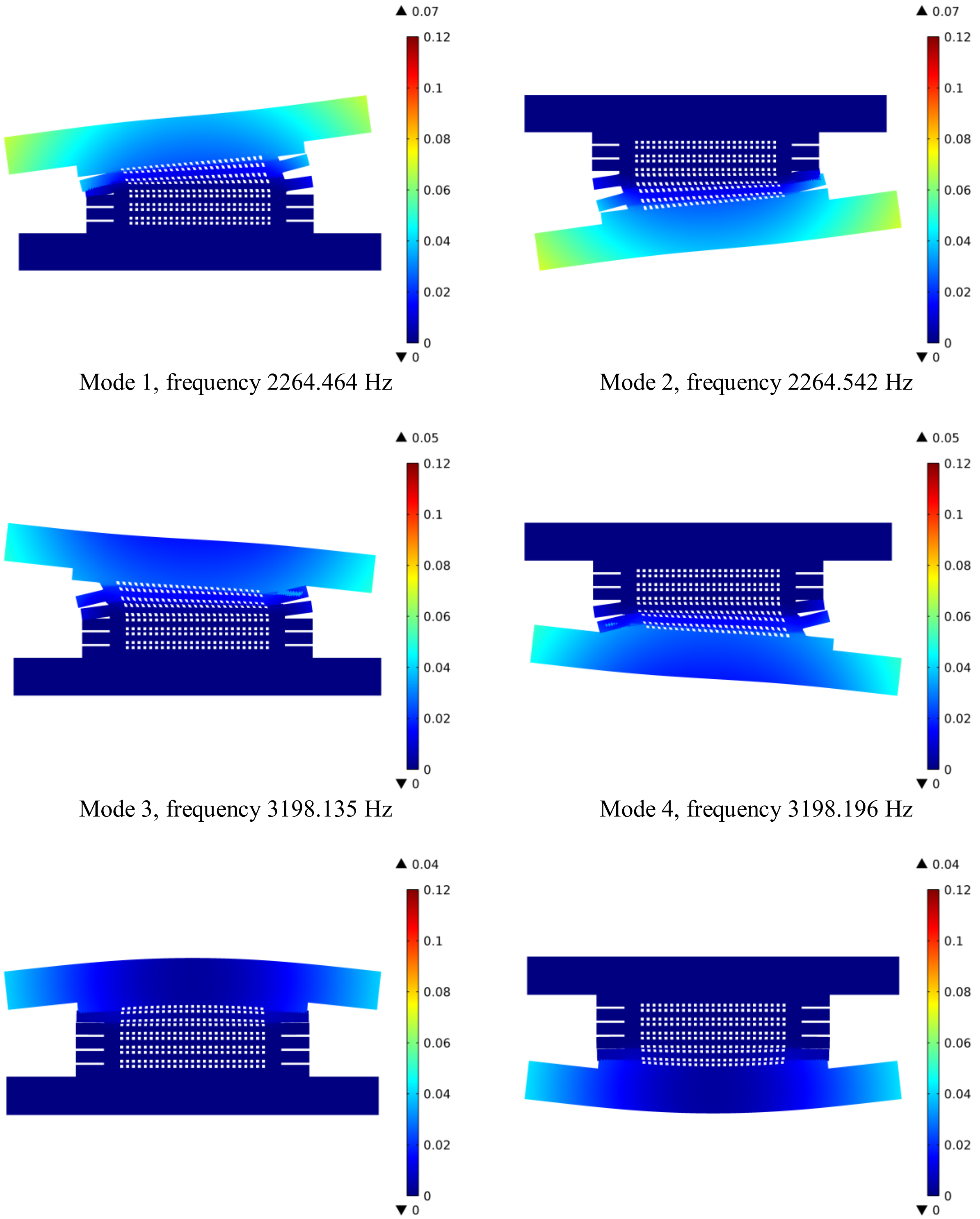

Mode 1, frequency 2264.464 Hz

Mode 2, frequency 2264.542 Hz

Mode 3, frequency 3198.135 Hz

Mode 4, frequency 3198.196 Hz

Mode 5, frequency 3823.293 Hz

Mode 6, frequency 3823.299 Hz

Figure 9. First six natural mode shapes with total displacement [nm]. (Current plates: Young's modulus = 209 GPa; Density = 7800 kg/m^3; Poisson's ratio = 0.25).

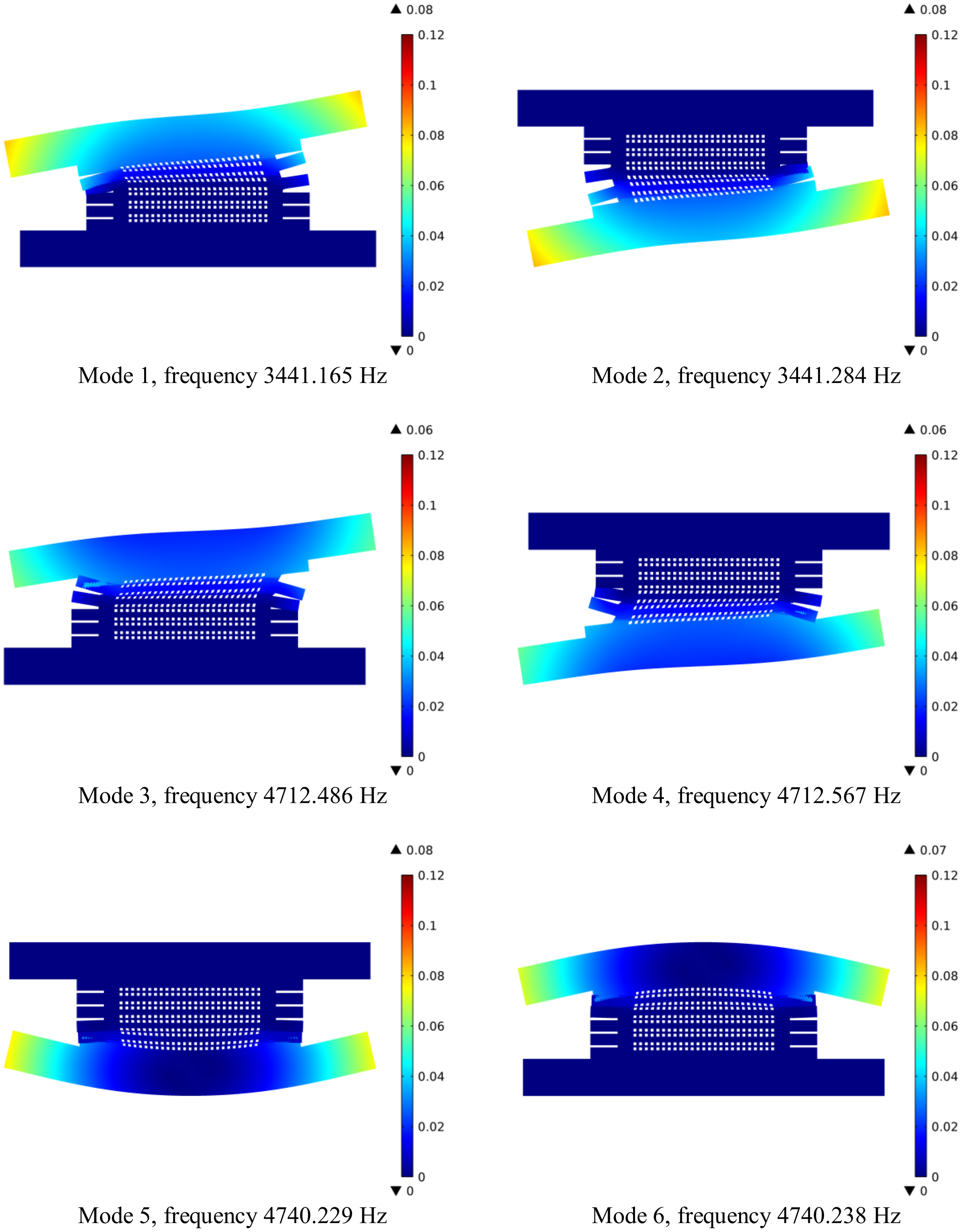

Figure 10. First six natural mode shapes with total displacement [nm]. (End plate (Aluminum):Young's modulus = 70 GPa; Density = 2700 kg/m^3; Poisson's ratio = 0.33).

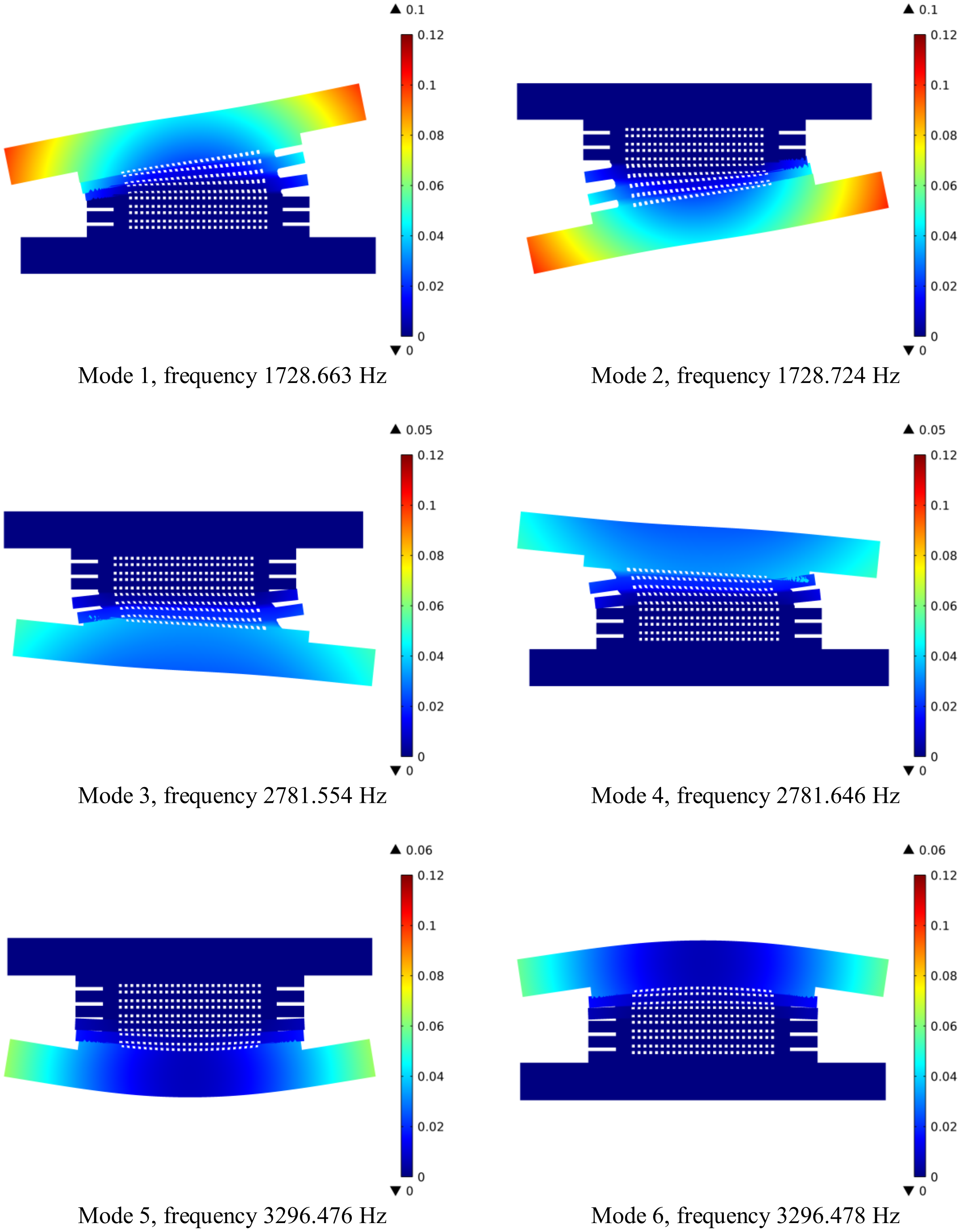

Figure 11. First six natural mode shapes with total displacement [nm]. (GDL and Gasket thicknesses = 0.5 mm).

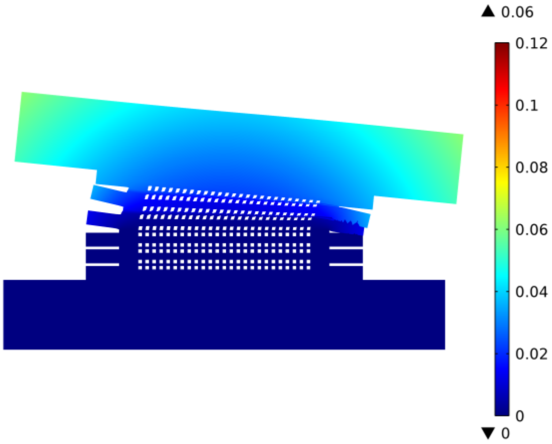

Mode 1, frequency 1798.373 Hz

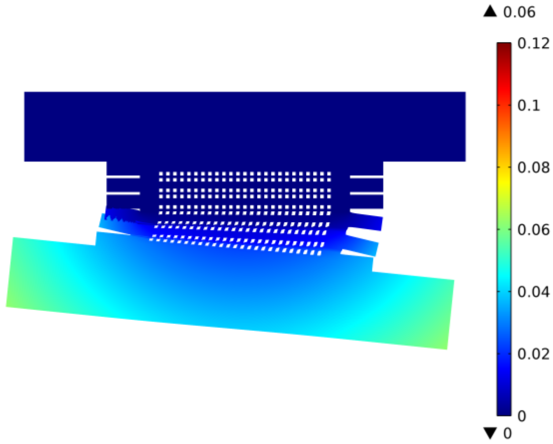

Mode 2, frequency 1798.455 Hz

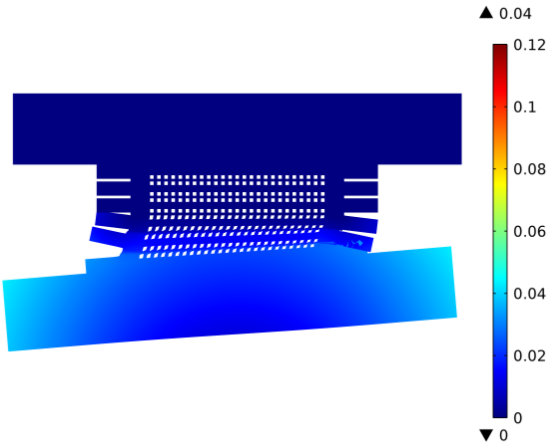

Mode 3, frequency 2797.372 Hz

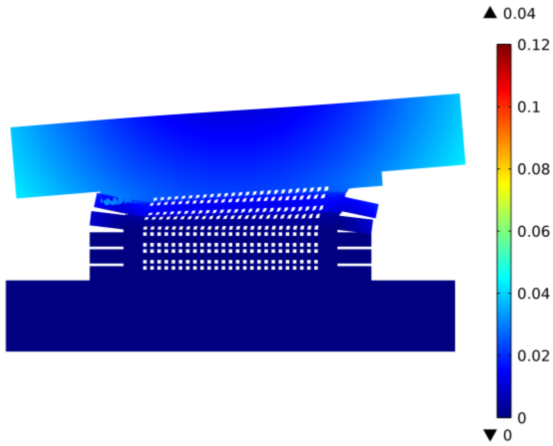

Mode 4, frequency 2797.680 Hz

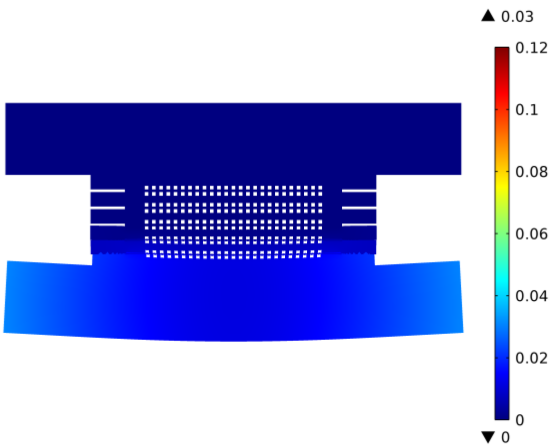

Mode 5, frequency 3935.895 Hz

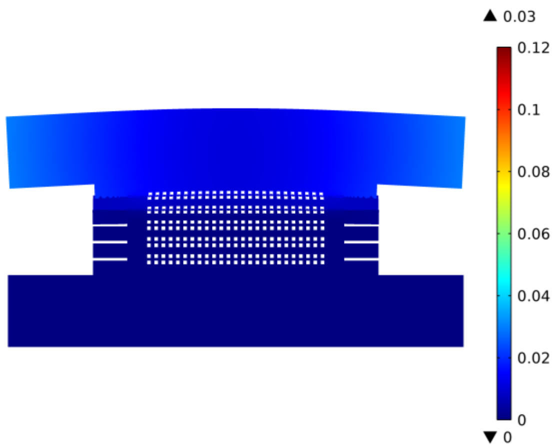

Mode 6, frequency 3936.008 Hz

Figure 12. First six natural mode shapes with total displacement [nm]. (End plate thickness = 20 mm).

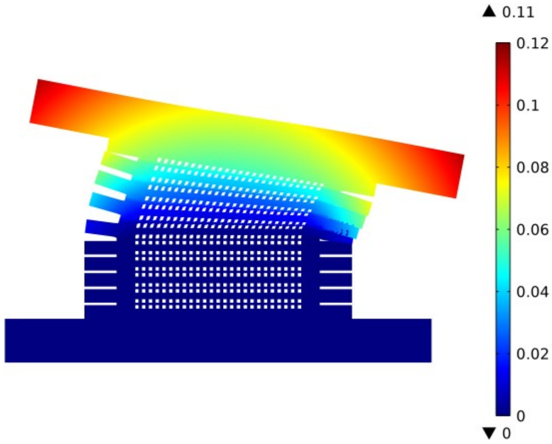

Mode 1, frequency 1523.228 Hz

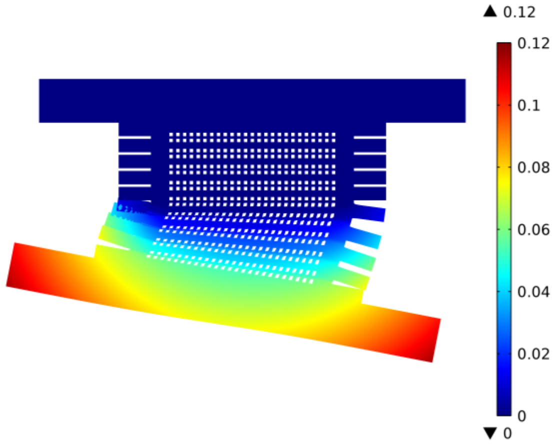

Mode 2, frequency 1523.248 Hz

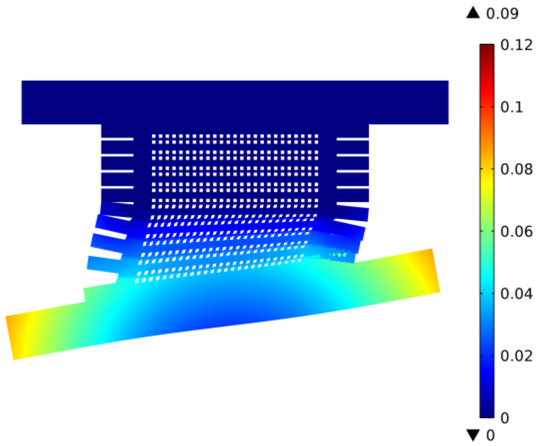

Mode 3, frequency 2409.492 Hz

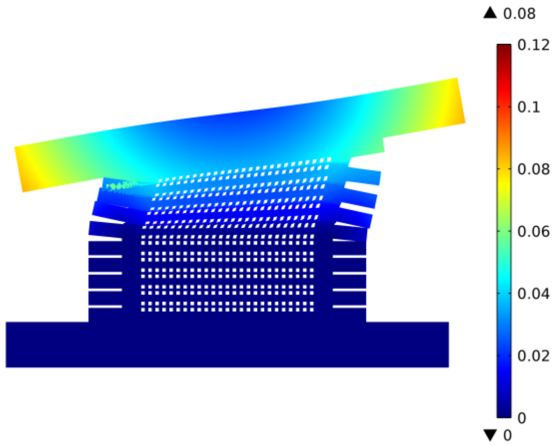

Mode 4, frequency 2409.536 Hz

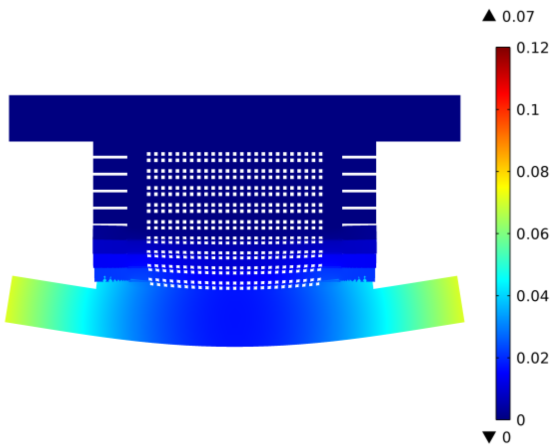

Mode 5, frequency 3190.672 Hz

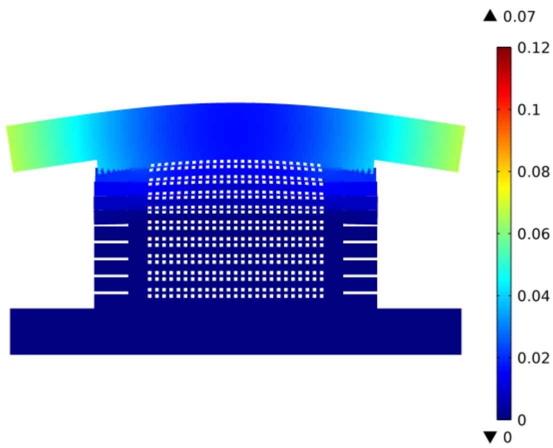

Mode 6, frequency 3190.694 Hz

Figure 13. First six natural mode shapes with total displacement [nm]. (Number of cells in the stack = 9).

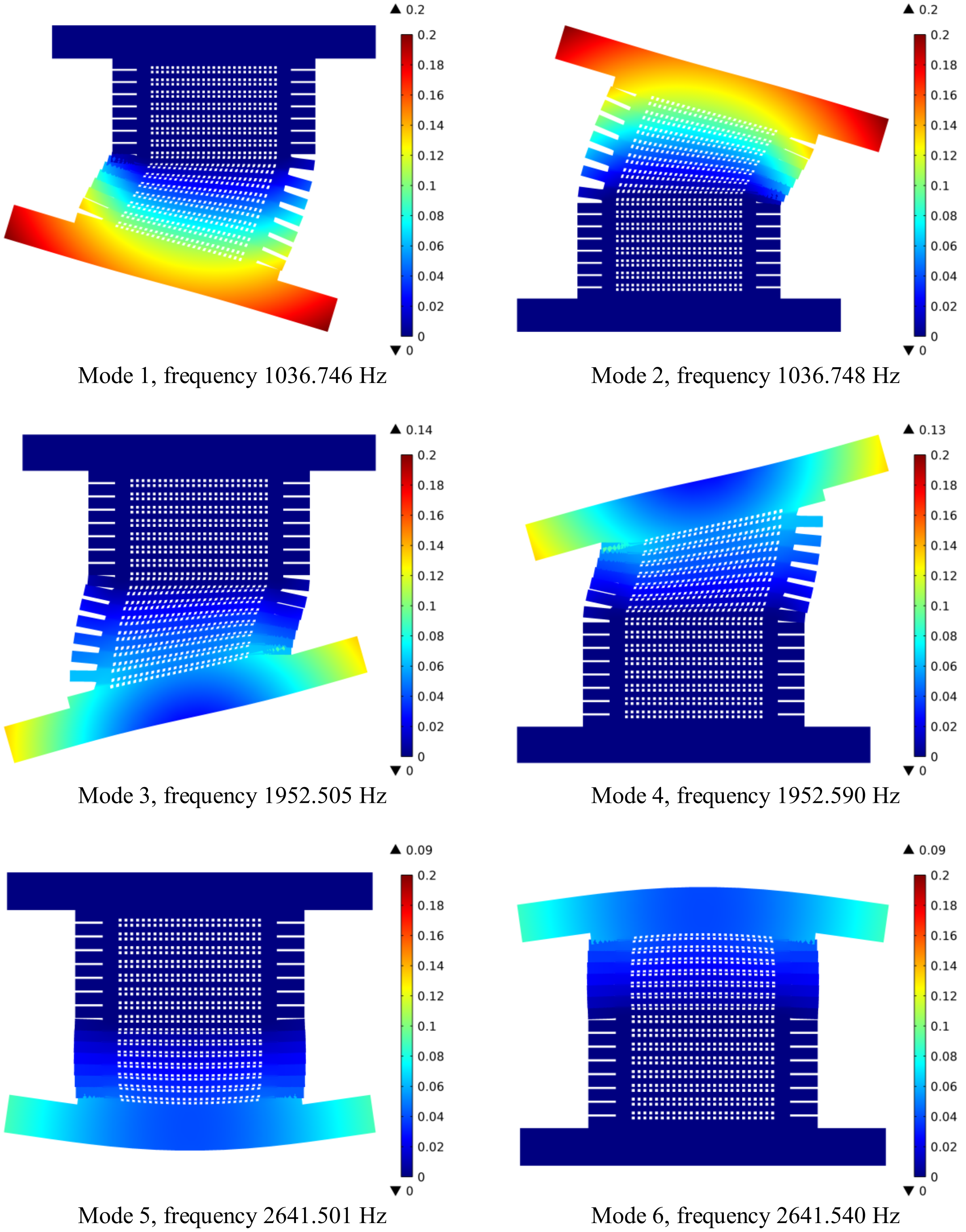

Figure 14. First six natural mode shapes with total displacement [nm]. (Number of cells in the stack = 15).

3.4. Effect of misalignment during assembly process

In practice, multiple single cells are usually connected in series to form a PEM fuel cell stack to provide the sufficient power and desired voltage. This configuration results in a high requirement of assembly accuracy for the adjacent bipolar plates. Otherwise, the assembly error will affect the perfect alignment of the adjacent bipolar plates and there will be an assembly position deviation, which leads to the assembly force transmitting asymmetrically and in turn makes the contact pressure distribution between the bipolar plate and MEA non-uniform [14]. Moreover, such assembly error brings an extra moment to the MEA, which may deform the MEA seriously and produce stress concentration even cracks [15]. Once the stress of MEA exceeds its yield strength, the plastic deformation will happen, and in turn, results in residual stresses in MEA after unloading, which are believed to be a significant contributor for the stress failure of MEA. Hence, it is very important to control the assembly error of the bipolar plate to a low level in order to maintain a proper pressure distribution and avoid stress failure of the MEA.

However, the assembly error for the PEM fuel cell stack has not received enough attention currently, and in particular manual assembly processes are still widely applied for most of the stacks, which results in large assembly errors of the bipolar plates. Furthermore, during the running of a PEM fuel cell stack, the unavoidable vibration may aggravate the assembly error, especially for the automotive application due to more vibrations [8]. In addition, for the PEM fuel cell stack of metallic bipolar plate, the bipolar plate exhibits larger manufacturing error because of its plastic characters (for example spring-back), which in turn makes the influence of assembly error more serious.

On one hand, the assembly error of bipolar plate should be controlled and decreased in order to improve the performance of the PEM fuel cell stack. On the other hand, based on the current assembly process and manufacturing process, it is very hard to control the assembly error to a very low level. And moreover if the assembly error required is too small, the assembly and manufacturing cost of the PEM fuel cell stack will increase dramatically, which is unacceptable and conflict with the cost reduction of the PEM fuel cell. Therefore, there is a need to investigate the effect of the assembly error of the bipolar plate on the contact behaviour of PEM fuel cell stack in order to guide the assembly process, and furthermore obtain a trade-off between the performance and the assembly accuracy.

An example result of the misalignment (the channel alignment of the bipolar plate on the anode side is not be in the perfect match of the channel on the cathode side) during the process of fuel cell stack assembly are shown in Figures 15 and 16.

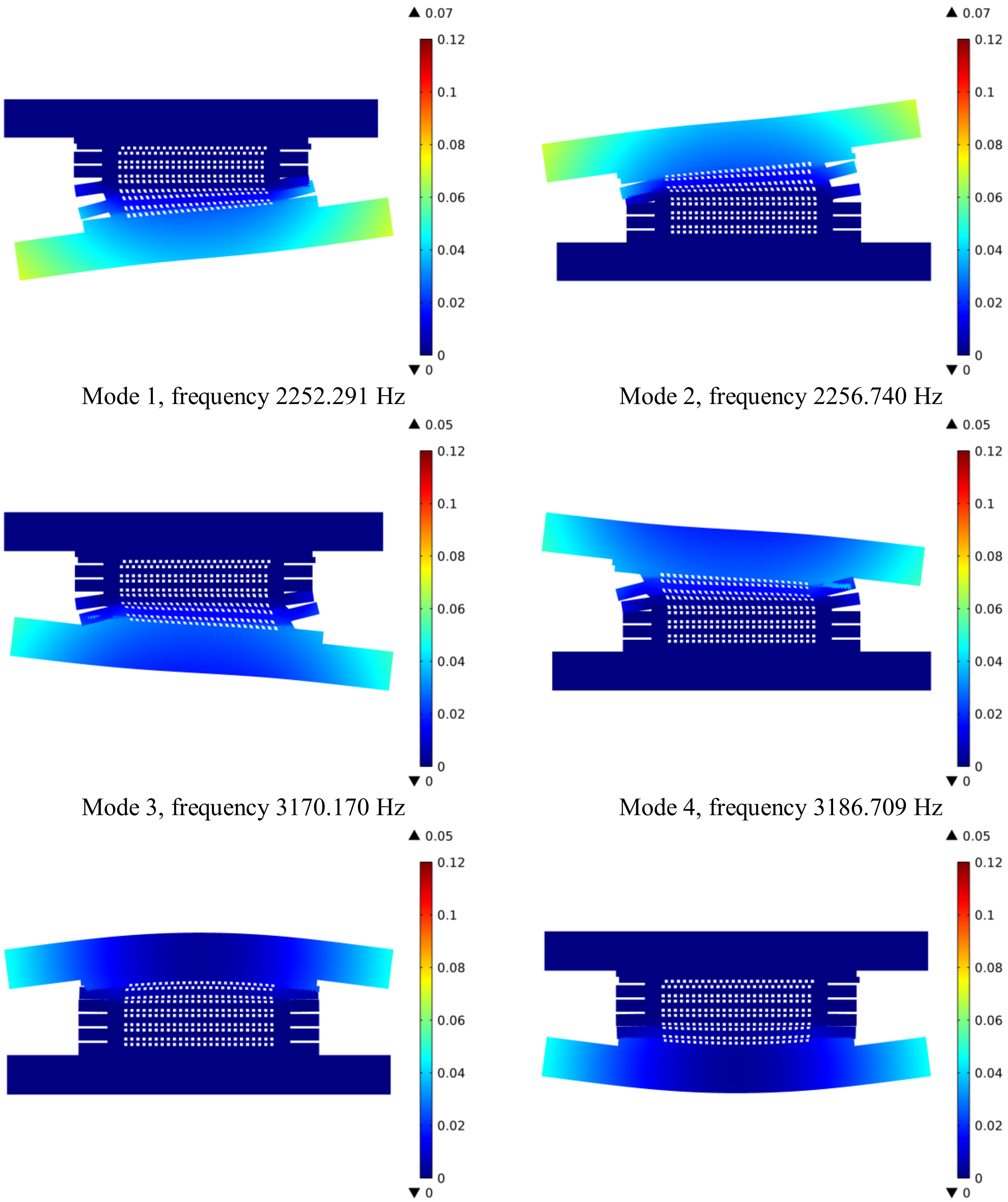

Mode 1, frequency 2252.291 Hz

Mode 2, frequency 2256.740 Hz

Mode 3, frequency 3170.170 Hz

Mode 4, frequency 3186.709 Hz

Mode 5, frequency 3682.988 Hz

Mode 6, frequency 3685.373 Hz

Figure 15. First six natural mode shapes with total displacement [nm]. (With assembly error: Type 1).

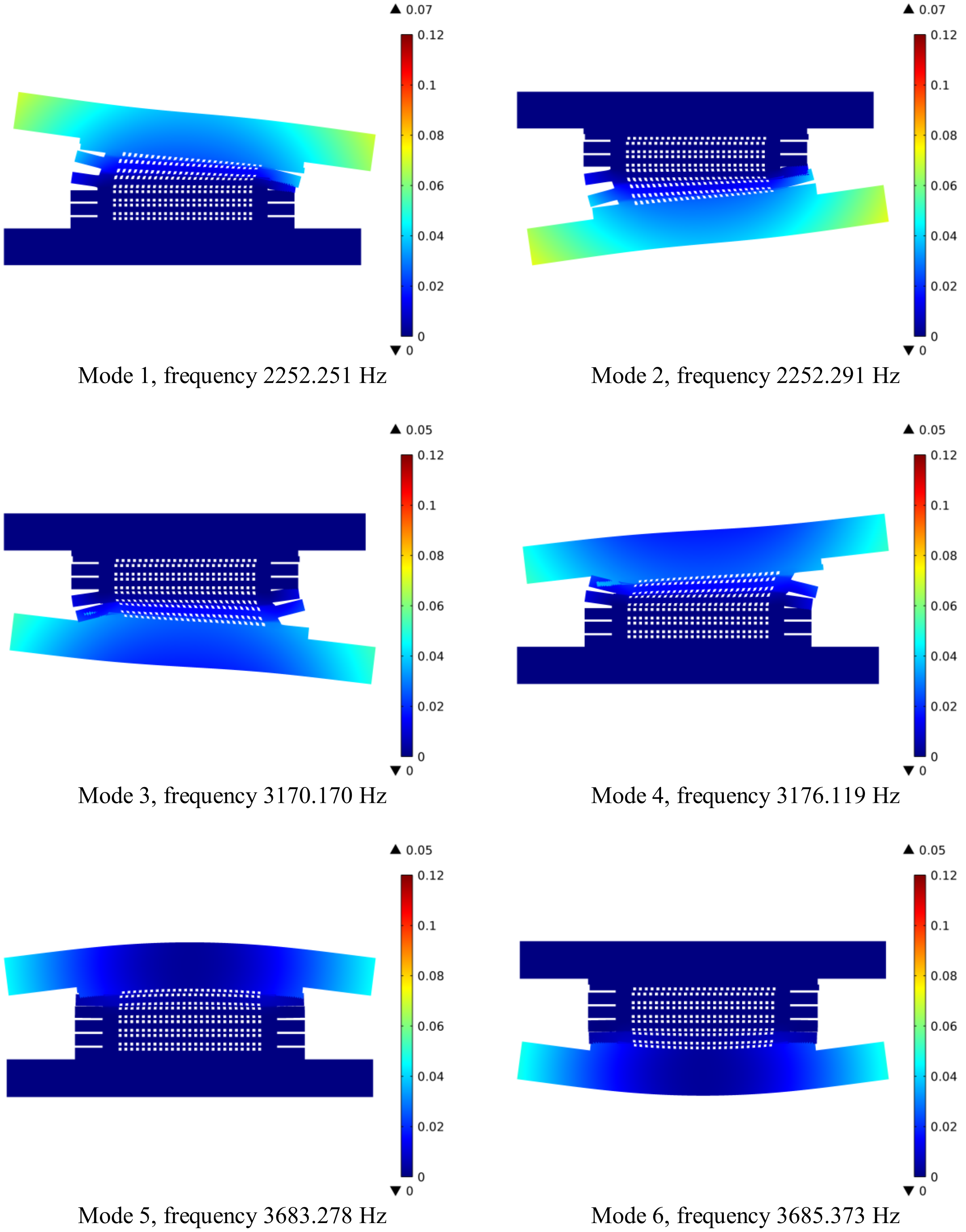

Figure 16. First six natural mode shapes with total displacement [nm]. (With assembly error: Type 2).

4. Conclusion

Vibration characteristics are required to understand the vibration behaviour of PEM fuel cell stack components such as the membrane, catalyst layer, gas diffusion layers, bi-polar plates, gasket, current plates, and end plates. Vibrating at resonance frequency can lead to the initiation and acceleration of defect formation, which may ultimately result in operational failure. Vibrations may exacerbate defects such as pinholes, cracks, and delamination, which can result in fuel crossover, leakage of fuel gas and coolant water, performance degradation, and reduced durability.

Natural frequencies and mode shapes of the PEM fuel cell stack are modelling using finite element methods (FEM). A parametric study is conducted to investigate how the natural frequency varies as a function of thickness, Young's modulus, and density for each component layer.

References

[1] Maher A.R. Sadiq Al-Baghdadi. CFD models for analysis and design of PEM fuel cells. Nova Science Publishers 2008, ISBN: 978160456-9971.

[2] Maher A.R. Sadiq Al-Baghdadi. CFD modeling and analysis of different novel designs of air-breathing PEM fuel cells. Nova Science Publishers 2010, ISBN: 9781608764891.

[3] Maher A.R. Sadiq Al-Baghdadi. PEM Fuel Cells Fundamentals, Modeling and Applications. International Energy and Environment Foundation 2013, ISBN: 9781481978231.

[4] Maher A.R. Sadiq Al-Baghdadi. PEM Fuel Cells - from Single Cell to Stack: Fundamentals, Modeling, Analysis, and Applications. International Energy and Environment Foundation 2015, ISBN: 9781505885644.

[5] Maher A.R. Sadiq Al-Baghdadi. A CFD study of hygro-thermal stresses distribution in PEM fuel cell during regular cell operation. Renewable Energy Journal 2009; 34(3): 674-682.

[6] Jaydeep Deshpande, Tapobrata Dey, Prakash C Ghosh. Effect of Vibrations on Performance of Polymer Electrolyte Membrane Fuel Cells. Energy Procedia 54, 2014, 756-762.

[7] Ahmed HEU, Banan R, Yu JW, Bazylak A, Free vibration analysis of a polymer electrolyte membrane fuel cell. J. Power Sources 2011, 196, 5520-5525.

[8] Roshanak Banan, Aimy Bazylak, Jean Zu. Effect of mechanical vibrations on damage propagation in polymer electrolyte membrane fuel cells. International journal of hydrogen energy 2013, 38, 14764-14772.

[9] N. Rajalakshmi, S. Pandien, K.S. Dhathathreyan, International Journal of Hydrogen Energy 2009, 34, pp.3833-3837.

[10] K. Ozgur, International ANSYS Conference Proceedings, 2004, Ch.1-11.

[11] M.C. Betournay, G. Bonnel, E. Edwardson, D. Paktunc, A. Kaujman, A.T. Lomma, Journal of Power Sources 2004, 134, pp.80-87.

[12] R. Bove, T. Malkow, A. Saturnio, G. Tsotridis, Journal of Power Sources 2008, 180, pp.452-460.

[13] Dong-hao Ye, Zhi-gang Zhan. A review on the sealing structures of membrane electrode assembly of proton exchange membrane fuel cells. Journal of power sources 2013, 231, pp.285-292.

[14] Dong'an Liu, Linfa Peng, Xinmin Lai. Effect of assembly error of bipolar plate on the contact pressure distribution and stress failure of membrane electrode assembly in proton exchange membrane fuel cell. Journal of power sources 2010, 195, pp.4213-4221.

[15] Dong'an Liu, Linfa Peng, Xinmin Lai. Effect of dimensional error of metallic bipolar plate on the GDL pressure distribution in the PEM fuel cell. International journal of hydrogen energy 2009, 34, pp.990-997.

